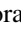


Thermocrystallization of lattice dipolar bosons coupled to a high-finesse cavityYaghmorassene Hebib ¹, Chao Zhang^{2,3,4,*}, Massimo Boninsegni⁵, and Barbara Capogrosso-Sansone¹¹*Department of Physics, Clark University, Worcester, Massachusetts 01610, USA*²*Department of Physics, Anhui Normal University, Wuhu, Anhui 241000, China*³*Department of Modern Physics, University of Science and Technology of China, Hefei, Anhui 230026, China*⁴*Hefei National Laboratory, University of Science and Technology of China, Hefei, Anhui 230088, China*⁵*Department of Physics, University of Alberta, Edmonton, Alberta, Canada, T6G 2H5*

(Received 14 February 2024; revised 28 March 2024; accepted 3 April 2024; published 9 May 2024)

Investigating finite-temperature effects on quantum phases is key to their experimental realization. Finite temperature and the interplay between quantum and thermal fluctuations can undermine properties and/or key features of quantum systems, but they can also bring about interesting phenomena. In this paper we present a comprehensive investigation of the finite-temperature phase diagram of two-dimensional lattice dipolar bosons coupled to a high-finesse optical cavity. Interestingly, we observe that checkerboard density-density correlations are enhanced at finite temperature. Indeed, we found that finite temperature drives a superfluid ground state into a normal state, which will then develop checkerboard order at higher temperatures. We show that this effect is solely due to the cavity-mediated interactions. We also confirm that the supersolid checkerboard phase survives for a wide range of filling factors up to a temperature scale of the order of half hopping amplitude, while the checkerboard diagonal order can survive up to temperatures of a few hopping amplitudes.

DOI: [10.1103/PhysRevB.109.174515](https://doi.org/10.1103/PhysRevB.109.174515)**I. INTRODUCTION**

The experimental realization of long-range interactions such as dipolar and cavity-mediated infinite-range interactions with ultracold gases [1–5] has opened up avenues for exploring intriguing quantum phases, novel collective behaviors, and unconventional many-body quantum states that were previously inaccessible. This has sparked a burgeoning interest in theoretical investigations of such systems [6,7]. With the first experimental realization of the Bose-Hubbard model with cavity-mediated interactions [3], quantum phases such as charge-density wave, superfluid, and supersolid were observed. Subsequently, a thorough numerical study of the same model confirmed the existence of such quantum phases [8]. Supersolid phases and a variety of charge-density waves were numerically investigated over a decade ago for purely repulsive dipolar bosons in a square lattice [9].

In Ref. [10], the authors studied the phase diagram of a system of lattice dipolar bosons coupled to high-finesse cavities in two dimensions. Unlike previous studies, this system encompasses both purely repulsive dipolar interactions, which follow a $1/r^3$ decay, and cavity-mediated infinite-range interactions. In its ground state, the system realizes superfluid, checkerboard solid, checkerboard supersolid, and incompressible phases. One of the main findings of [10] is that the checkerboard supersolid phase can exist across a broader range of particle densities compared to the case with no cavity-mediated interactions. These unbiased numerical findings suggest the practical feasibility of achieving supersolids

using current achievable fillings in polar molecule experiments.

A key question for experimental realization of quantum phases is the role of thermal fluctuations. Finite temperature, and the interplay between quantum and thermal fluctuations can undermine properties and/or key features of quantum systems but also bring upon interesting phenomena. In particular, the robustness of the liquid phase at low temperature is crucially underlain by quantum-mechanical exchanges in Bose systems. Indeed, it has been shown [11] that even condensed ^4He , long believed to remain a fluid down to zero temperature due to atomic zero-point motion alone, would in fact undergo thermocrystallization at finite temperature, in the absence of quantum statistics (i.e., if ^4He atoms were distinguishable quantum particles). A similar effect of reentrance of crystalline order at finite temperature, arising as exchanges are suppressed with the reduction of the thermal wavelength, has also been predicted for small clusters of parahydrogen, which undergo “quantum melting” as the temperature $T \rightarrow 0$ [12,13]. Moreover, this interesting behavior has also been observed in experiments with ultracold dipolar gases. In Ref. [14] the authors observe that density-density correlations are enhanced at finite temperature.

In this paper we study the finite-temperature phase diagram of dipolar bosons coupled to a high-finesse cavity and trapped in a square lattice. By means of a path-integral Monte Carlo, we perform simulations of the extended Bose-Hubbard model and determine critical temperatures for the disappearance of diagonal and off-diagonal order. Interestingly, we observe that checkerboard density-density correlations are enhanced at finite temperature. Indeed, finite temperature drives a superfluid ground state into a normal state, which will then develop

*chaozhang@ahnu.edu.cn

checkerboard order at higher temperatures. This paper is organized as follows: In Sec. II we introduce the Hamiltonian of the system. In Sec. III we discuss various phases and the corresponding order parameters. In Sec. IV we present the finite-temperature phase diagrams of the system for fixed values of the onsite and cavity-mediated interactions; we outline our conclusions in Sec. V.

II. HAMILTONIAN

We consider a system of dipolar bosons trapped in a square optical lattice and coupled to a high-finesse optical cavity. The dipoles are aligned perpendicular to the optical lattice plane, ensuring that the dipolar interaction is purely repulsive and isotropic. Within the single-band approximation, this system is governed by the following extended Bose-Hubbard Hamiltonian [3,15]:

$$H = -t \sum_{\langle ij \rangle} a_i^\dagger a_j + \frac{U_s}{2} \sum_i n_i(n_i - 1) + \frac{V_{\text{dip}}}{2} \sum_{i,j} \frac{n_i n_j}{r_{ij}^3} - \frac{V_{\text{ca}}}{L^2} \left(\sum_{i \in e} n_i - \sum_{j \in o} n_j \right)^2 - \mu \sum_i n_i. \quad (1)$$

Here, the first term represents the kinetic energy, characterized by hopping amplitude t . The summation over $\langle ij \rangle$ signifies that the sum is taken over the nearest-neighboring sites. The operators a_i^\dagger and a_i are the bosonic creation and annihilation operators, respectively, obeying the standard bosonic commutation relations. The second term in the Hamiltonian describes the on-site repulsive interaction with a strength U_s . In this context, $n_i = a_i^\dagger a_i$ denotes the number operator for the particles at site i . The third term is the dipolar interaction between the sites, with dipolar interaction strength V_{dip} and $r_{ij} = |r_i - r_j|$ as the relative distance between sites i and j . The fourth term is the cavity-mediated long-range interaction, characterized by the interaction strength V_{ca} , with the summations over $i \in e$ and $j \in o$ indicating sums over even and odd lattice sites, respectively. The final term is the chemical potential μ .

III. METHOD AND ORDER PARAMETERS

The results we will present in the following are based on the path-integral quantum Monte Carlo by the worm algorithm [16]. We consider a square lattice of sizes $L = 16, 20, 24, 30$ (we set our unit of length to be the lattice step, $a = 1$). We impose periodic boundary conditions in both spatial dimensions. To properly account for the long-range dipolar interaction, Ewald summation was utilized. The inverse temperature is denoted by $\beta = 1/T$ (in our units, the Boltzmann constant $k_B = 1$).

To characterize the various phases, we calculated superfluid density ρ_s and structure factor $S(\pi, \pi)$. The superfluid density is calculated in terms of winding numbers [17]:

$$\rho_s = \frac{\langle \mathbf{W}^2 \rangle}{DL^{D-2}\beta}, \quad (2)$$

where $\langle \mathbf{W}^2 \rangle = \langle \sum_{i=1}^D W_i^2 \rangle$ is the expectation value of winding number square, D is the dimension of the system (here

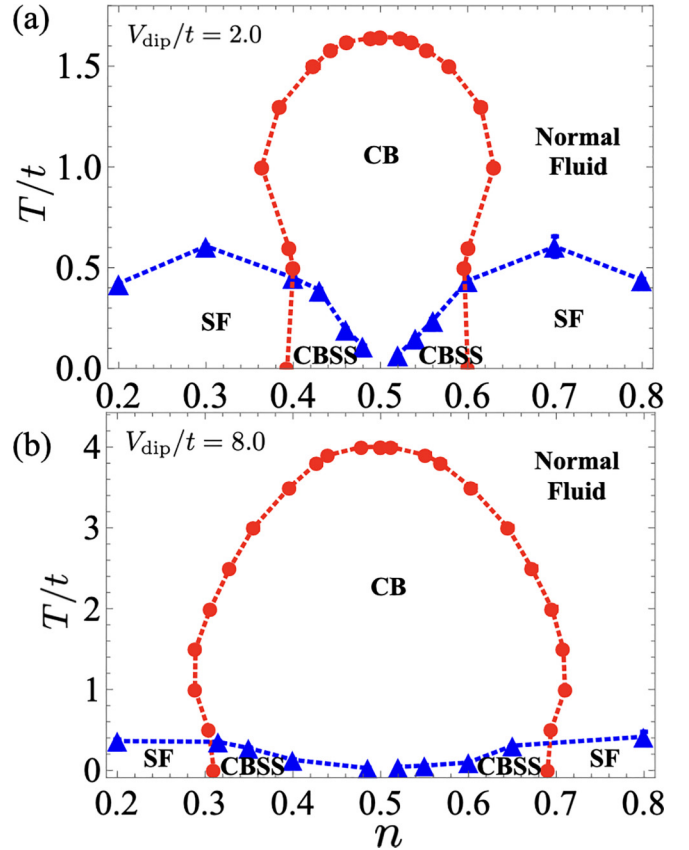


FIG. 1. Critical temperatures for the disappearance of off-diagonal long-range order (blue triangles) and diagonal long-range order (red circles) as a function of filling factor n at dipolar interaction $V_{\text{dip}}/t = 2$ (a) and $V_{\text{dip}}/t = 8$ (b).

$D = 2$), L is the linear system size, and β is the inverse temperature. The structure factor characterizes diagonal long-range order and is defined as

$$S(\mathbf{k}) = \frac{\sum_{\mathbf{r}, \mathbf{r}'} \exp[i\mathbf{k}(\mathbf{r} - \mathbf{r}') \langle n_{\mathbf{r}} n_{\mathbf{r}'} \rangle]}{N}, \quad (3)$$

with N the particle number, and \mathbf{k} is the reciprocal lattice vector. Here, $\mathbf{k} = (\pi, \pi)$ to identify a checkerboard density pattern.

IV. RESULTS AND DISCUSSION

In the following we work at filling factor $n = N/L^2 < 1$, and fixed values of $U_s/t = 20.0$ and $V_{\text{ca}}/t = 2.0$. Finite cavity-mediated interaction favors a density wave between even and odd sites. At $T = 0$ and for $V_{\text{dip}} \gtrsim 1.13t$, model (1) features a checkerboard (CB) solid phase at $n = 0.5$. Upon doping the CB solid with particles or holes, the system enters a CB supersolid phase (CBSS). For large enough doping, density-density correlations are eventually destroyed via a second-order phase transition belonging to the $(2+1)$ Ising universality class, leaving the system in a superfluid (SF) phase. For $V_{\text{dip}} \lesssim 1.13t$, the system is a SF for any n . For $V_{\text{dip}} \gtrsim 10t$, other incompressible phases are stabilized. Here, we do not consider these values of dipolar interaction. For more details, see [10].

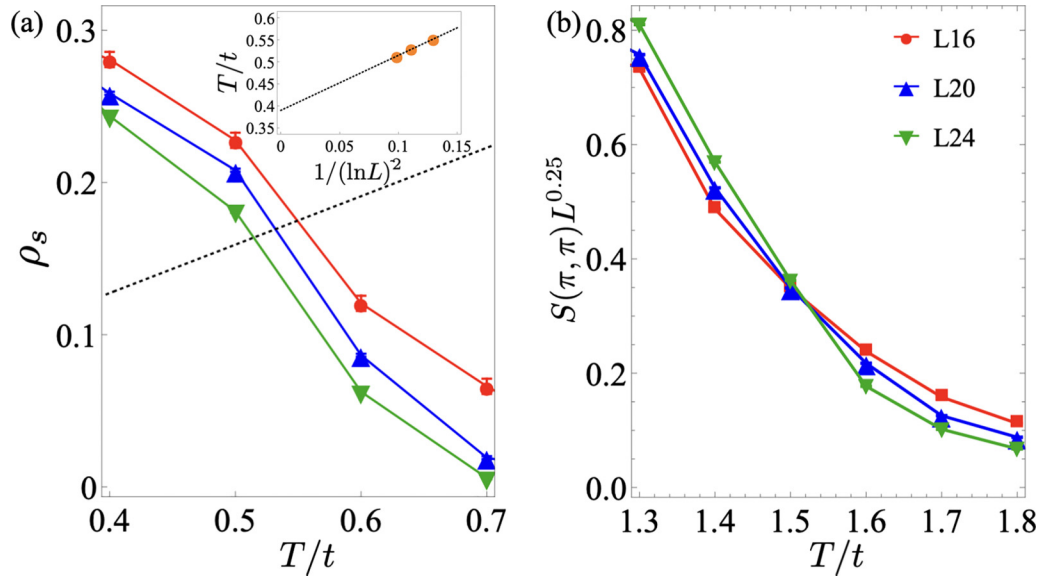


FIG. 2. $V_{\text{dip}}/t = 2$ and $n = 0.43$. Upon increasing the temperature, thermal fluctuations destroy the checkerboard supersolid phase. First, superfluidity is destroyed via a Kosterlitz-Thouless phase transition, and the checkerboard supersolid becomes a liquid-like phase with finite density-density correlations. Then, checkerboard density-density correlations disappear via a two-dimensional Ising transition and the system is a normal fluid. In (a) we show ρ_s as a function of T/t for $L = 16$ (red), 20 (blue), 24 (green). The dotted line is $T/t\pi$. Inset: intersection points between the $T/t\pi$ line and the ρ_s vs T/t curves for each L are used to extract $T_c/t \sim 0.39 \pm 0.01$. (b) Scaled structure factor with $2\beta/\nu = 0.25$ for $L = 16, 20, 24$. The crossing determines the critical temperature $T_c/t = 1.52 \pm 0.02$.

In Fig. 1 we show the finite T phase diagram for two values of dipolar interaction, $V_{\text{dip}}/t = 2$ (a) and $V_{\text{dip}}/t = 8$ (b). Superfluidity disappears via a Kosterlitz-Thouless (KT) type transition [18] (blue triangles in Fig. 1), while the CB order disappears via a two-dimensional Ising-type transition (red circles). Therefore, we can associate two critical temperatures, $T_{\text{KT,SS}}$ and $T_{\text{CB,SS}}$, corresponding to the disappearance of off-diagonal and diagonal long-range order of the CBSS. Other than for n values in the vicinity of the SF-CBSS transition at zero temperature, $T_{\text{KT,SS}} < T_{\text{CB,SS}}$. This means that the off-diagonal order of the CBSS disappears first so that the system enters a liquidlike, compressible phase with finite density-density correlations.

In Fig. 2 we show details on how critical temperatures are calculated. In Fig. 2(a) we show the procedure followed for KT transition temperatures. The superfluid density ρ_s is plotted as a function of T/t for $L = 16, 20, 24$ at $V_{\text{dip}}/t = 2$ and $n = 0.43$. In the thermodynamic limit, a universal jump is observed at the critical temperature given by $\rho_s(T_c) = 2mk_B T_c / \pi \hbar^2$. Here, m is the effective mass in the lattice, $m = \hbar^2 / 2ta^2$. In a finite-size system this jump is smeared out as shown in Fig. 2(a). To extract the critical temperature in the thermodynamic limit, we apply finite-size scaling to $T_c(L)$. From renormalization-group analysis one finds $T_c(L) = T_c(\infty) + \frac{c}{\ln^2(L)}$, where c is a constant and $T_c(L)$ is determined from $\rho_s(T_c, L) = 2mk_B T_c / \pi \hbar^2$ [17,19,20]. The dotted line in Fig. 2(a) corresponds to $\rho_s = T/t\pi$ ($\hbar = 1$, $k_B = 1$, lattice step $a = 1$). Its intersection points with each ρ_s vs T/t curve are used to find T_c as shown in the inset. Here, we find $T_c/t = 0.39 \pm 0.01$. Above this temperature the system is in a liquidlike phase with finite density-density correlations. The density-density correlations will eventually disappear via

a two-dimensional Ising transition. In Fig. 2(b) we use standard finite-size scaling and plot the scaled structure factor $S(\pi, \pi)L^{2\beta/\nu}$, with $2\beta/\nu = 0.25$ as a function of T/t for $L = 16, 20, 24$. The crossing indicates a critical temperature $T_c/t = 1.52 \pm 0.02$.

Interestingly, the transition line for disappearance of diagonal order features a reentrant behavior so that the system develops density-density correlations at densities for which

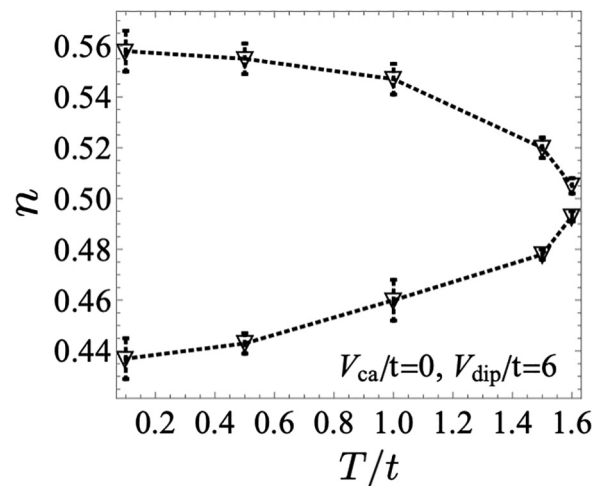


FIG. 3. CB density-density correlations are finite inside the lobe and nonexistent outside the lobe. In the absence of cavity-mediated interactions, no reentrant behavior is observed. Transition points have been determined using standard finite-size scaling arguments as discussed in Fig. 2(b), with the difference that here we have scanned through densities at fixed T rather than the opposite, as shown in Fig. 2(b).

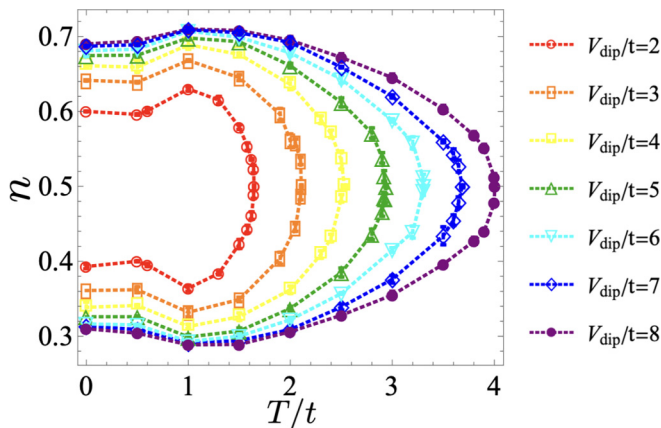


FIG. 4. Transition lines for disappearance of CB solid order at $V_{\text{dip}} = 2$ (blue), 3 (yellow), 4 (green), 5 (purple), 6 (black), 7 (red), and 8 (magenta). All curves exhibit a reentrant behavior. Transition points have been determined using standard finite-size scaling arguments as discussed in Fig. 2(b), with the difference that here we have scanned through densities at fixed T rather than the opposite, as shown in Fig. 2(b).

the ground state is SF. We notice that the onset of this reentrant behavior is concurrent with the disappearance of superfluidity. More specifically, in the proximity of the CBSS-SF transition at zero temperature, there exists a range of densities for which the ground state is a SF. Upon increasing temperature, the SF state disappears through a KT transition in favor of a normal fluid, i.e., a state where quantum statistics has become less relevant. By further increasing T , the normal fluid develops CB-type density-density correlations. This effect is solely due to the cavity-mediated interaction. This interaction mimics an external pinning potential and discourages exchanging of indistinguishable particles. As a result, the system behaves more classical-like and supports density-density correlations [11]. In Fig. 3 we consider the case of no cavity-mediated interaction, for which the CB order exists at $V_{\text{dip}}/t \gtrsim 4.75$ [21]. Here, we plot the n vs T/t line at $V_{\text{dip}}/t = 6$, for which CB density correlations disappear so that outside the lobe the CB density-density correlations are nonexistent. We do not observe any reentrant behavior. Finally, in Fig. 4 we plot the transition lines for the disappearance of CB density-density correlations for a range of V_{dip}/t from the onset of the CB order to before the onset of a variety of other incompressible phases at $T = 0$ [10]. For each fixed V_{dip}/t , CB order exists inside the corresponding lobe. We notice that the reentrant behavior is always observed, though it is more pronounced at lower values of V_{dip}/t where cavity-mediated interactions are more prominent. As expected, at larger values of V_{dip}/t , CB order survives at larger temperatures. These results confirm that at finite T , CB order still exists for filling factors as low as $n \sim 0.29$. Therefore this solid order has the potential to be observed with ultracold polar molecules, for which currently achievable filling factors are still pretty low, $n \sim 0.25$ – 0.3 [22,23].

V. CONCLUSION

In this work we investigated the effects of finite temperature on a system of lattice dipolar bosons coupled to a high-finesse optical cavity. We found that there exists a range of densities for which the system undergoes thermocrystallization above the KT transition. In other words, upon increasing temperature, a SF state first becomes a normal liquid and then develops density-density correlations. This effect is due to finite cavity-mediated interactions which suppress exchanges of identical particles and hence favoring density-density correlations.

The results presented in this paper should be within experimental reach in the near future. Experiments with lattices gases coupled to a high-finesse cavity have already been realized [3]. These setups should be able to be extended to dipolar gases of magnetic atoms such as Cr, Er, and Dy [24], and polar molecules such as Er_2 , K Rb , NaK, NaRb [25,26]. Interaction strengths and tunneling are all highly controllable with the external fields. The number of particles can be controlled by using different evaporation depths. Different filling factors can also be achieved within the same experiment in the presence of an external trapping potential V_i^{ext} . In the local density approximation, which is actually a local chemical potential approximation, the density at site i is identified with the density of the homogeneous system, with a local effective chemical potential given by $\mu - V_i^{\text{ext}}$. The temperatures required to observe thermocrystallization are of the order of the hopping amplitude. These temperatures can be achieved in current experiments. We notice that the signature of thermocrystallization in the presence of the harmonic trap would be an increase in the region of space where density-density correlations are finite as the temperature is increased. Density-density correlations can be observed with the quantum gas microscope (see, e.g., [27]).

We also observe that checkerboard-type density-density correlations exist at finite temperature for filling factors as low as $n \sim 0.29$, which is close to what is currently achievable in experiments with cold polar molecules. Moreover, recently, the first Bose-Einstein condensate of dipolar molecules in their ground state has been achieved [28]. This breakthrough opens the way to achieve larger filling factors, for which density-density correlations are more robust, of polar molecules in optical lattices.

ACKNOWLEDGMENTS

C.Z. acknowledges support from the National Natural Science Foundation of China (NSFC) under Grants No. 12204173, No. 12275263, and No. 12275002, the Innovation Program for Quantum Science and Technology (under Grant No. 2021ZD0301900), and the University Annual Scientific Research Plan of Anhui Province under Grant No. 2022AH010013. M.B. acknowledges support from the Natural Sciences and Engineering Research Council of Canada. The computing for this project was performed at the cluster at Clark University.

[1] L. Chomaz, I. Ferrier-Barbut, F. Ferlaino, B. Laburthe-Tolra, B. L. Lev, and T. Pfau, *Rep. Prog. Phys.* **86**, 026401 (2022).

[2] S. A. Moses, J. P. Covey, M. T. Miecinkowski, D. S. Jin, and J. Ye, *Nat. Phys.* **13**, 13 (2017).

- [3] R. Landig, L. Hruby, N. Dogra, M. Landini, R. Mottl, T. Donner, and T. Esslinger, *Nature* **532**, 476 (2016).
- [4] F. Mivehvar, F. Piazza, T. Donner, and H. Ritsch, *Adv. Phys.* **70**, 1 (2021).
- [5] H. Ritsch, P. Domokos, F. Brennecke, and T. Esslinger, *Rev. Mod. Phys.* **85**, 553 (2013).
- [6] C. Trefzger, C. Menotti, B. Capogrosso-Sansone, and M. Lewenstein, *J. Phys. B: At. Mol. Opt. Phys.* **44**, 193001 (2011).
- [7] N. Defenu, T. Donner, T. Macrì, G. Pagano, S. Ruffo, and A. Trombettoni, *Rev. Mod. Phys.* **95**, 035002 (2023).
- [8] T. Flottat, L. de Forges de Parny, F. Hébert, V. G. Rousseau, and G. G. Batrouni, *Phys. Rev. B* **95**, 144501 (2017).
- [9] B. Capogrosso-Sansone, C. Trefzger, M. Lewenstein, P. Zoller, and G. Pupillo, *Phys. Rev. Lett.* **104**, 125301 (2010).
- [10] Y. Hebib, C. Zhang, J. Yang, and B. Capogrosso-Sansone, *Phys. Rev. A* **107**, 043318 (2023).
- [11] M. Boninsegni, L. Pollet, N. Prokof'ev, and B. Svistunov, *Phys. Rev. Lett.* **109**, 025302 (2012).
- [12] F. Mezzacapo and M. Boninsegni, *Phys. Rev. Lett.* **97**, 045301 (2006).
- [13] F. Mezzacapo and M. Boninsegni, *Phys. Rev. A* **75**, 033201 (2007).
- [14] J. Sánchez-Baena, C. Politi, F. Maucher, F. Ferlino, and T. Pohl, *Nat. Commun.* **14**, 1868 (2023).
- [15] N. Dogra, F. Brennecke, S. D. Huber, and T. Donner, *Phys. Rev. A* **94**, 023632 (2016).
- [16] N. Prokof'ev, B. Svistunov, and I. Tupitsyn, *Phys. Lett. A* **238**, 253 (1998).
- [17] D. M. Ceperley and E. L. Pollock, *Phys. Rev. B* **39**, 2084 (1989).
- [18] J. M. Kosterlitz and D. J. Thouless, *J. Phys. C* **6**, 1181 (1973).
- [19] D. R. Nelson and J. M. Kosterlitz, *Phys. Rev. Lett.* **39**, 1201 (1977).
- [20] J. M. Kosterlitz, *J. Phys. C* **7**, 1046 (1974).
- [21] D. Grimmer, A. Safavi-Naini, B. Capogrosso-Sansone, and G. Söyler, *Phys. Rev. A* **90**, 043635 (2014).
- [22] S. A. Moses, J. P. Covey, M. T. Miecnikowski, B. Yan, B. Gadway, J. Ye, and D. S. Jin, *Science* **350**, 659 (2015).
- [23] L. Reichsöllner, A. Schindewolf, T. Takekoshi, R. Grimm, and H.-C. Nägerl, *Phys. Rev. Lett.* **118**, 073201 (2017).
- [24] L. Chomaz, I. Ferrier-Barbut, F. Ferlino, B. Laburthe-Tolra, B. L. Lev, and T. Pfau, *arXiv:2201.02672*.
- [25] J. L. Bohn, A. M. Rey, and J. Ye, *Science* **357**, 1002 (2017).
- [26] L. Christakis, J. S. Rosenberg, R. Raj, S. Chi, A. Morningstar, D. A. Huse, Z. Z. Yan, and W. S. Bakr, *arXiv:2207.09328*.
- [27] L. Su, A. Douglas, M. Szurek, R. Groth, S. F. Ozturk, A. Krahn, A. H. Hébert, G. A. Phelps, S. Ebadi, S. Dickerson, F. Ferlino, O. Marković, and M. Greiner, *Nature* **622**, 724 (2023).
- [28] N. Bigagli, W. Yuan, S. Zhang, B. Bulatovic, T. Karman, I. Stevenson, and S. Will, *arXiv:2312.10965*.